



Resolvent-based analysis of streaks in turbulent jets

Petrônio A. S. Nogueira and André V. G. Cavalieri

Divisão de Engenharia Aeronáutica, Instituto Tecnológico de Aeronáutica, Brazil

Oliver T. Schmidt

Department of Mechanical and Aerospace Engineering, University of California, San Diego, USA

Peter Jordan and Vincent Jaunet

Institut Pprime, CNRS–University of Poitiers–ENSMA, Poitiers, France

Ethan Pickering, Georgios Rigas and Tim Colonius

Department of Mechanical Engineering, California Institute of Technology, Pasadena, USA

Large scale, elongated structures, similar those ones widely studied in wall-bounded flows, are also present in turbulent jets. Several characteristics of these streaks can be identified via reduced order models such as resolvent analysis. The present work involves a resolvent-based study of these structures in turbulent jets. We focus on obtaining the optimal forcing that generates these energetic coherent structures. Results are compared with experimental data post-processed using spectral proper orthogonal decomposition, allowing us to draw conclusions about the nature of the non-linear forcing, since the two analyses should provide equivalent results if this term is modelled as spatially white. By identifying streaks in a global framework, we expect to better understand the mechanism by which they are generated.

I. Introduction

COHERENT structures have been studied in turbulent flows in several frameworks. In turbulent jets, the identification of hydrodynamic wavepackets, whose spatial evolution is largely controlled by the Kelvin-Helmholtz instability, led to several important conclusions regarding jet noise [1, 2]. For wall-bounded turbulence, researchers have been focusing on streamwise elongated structures in the near-wall region, called streaks, that play an important role in the dynamics of these kinds of flows [3], especially in terms of the turbulent kinetic energy production process [4]. These streaks are forced by streamwise vortices in a self-sustaining process that has been proposed as one of the foundations of turbulence dynamics [5–8]. Farther from the wall, similar streaky structures are also observed; these are referred to as superstructures [9] and are also thought to result from a similar self-sustaining process [10]. Elongated streaky structures, similar to those ubiquitous in wall-bounded turbulence, have recently been found in turbulent jets [11], and their characteristics greatly resemble superstructures found in turbulent boundary layers.

The presence of streaks in shear flows is due to the lift-up effect. This phenomenon was first studied by Ellingsen & Palm [12], who analysed the stability of homogeneous sheared flow, showing that disturbances can here be amplified by a linear, non-modal mechanism. This phenomenon tends to create streamwise elongated, alternating high-low streamwise velocity regions over the span, coupled with streamwise vortices; these transfer momentum from high to low velocity regions (when a positive streak occurs), the opposite occurring for a negative streak. Previous studies have identified this phenomenon in several confined sheared flows in the locally parallel framework [13, 14], and three dimensional computations confirm this behaviour for spatially evolving wall-bounded flows [15–17].

Several methods can be used to analyse the dynamics of streaks and streamwise vortices in wall-bounded flows. One of them, described in previous work [14, 18, 19], focuses on finding optimal forcing of the linearised Navier-Stokes system. This forcing will be related to the most amplified structure in the flow, leading to relevant information about how it is generated and, consequently, how it might be damped. Moreover, resolvent modes have a direct relationship with energetic structures observed experimentally; in fact, the response modes provided by resolvent analysis should be exactly equal to those obtained by spectral proper orthogonal decomposition of experimental data, if the forcing is white noise in space [20]. Other approaches can also be used for this problem. For instance, transient growth analysis [14], focuses on finding initial disturbance that will be most amplified in the flow, resulting in conclusions about the time evolution of these structures. Both analyses have been used in the identification of streaks in turbulent jets [11], using the locally parallel framework, focusing on streamwise wavenumber $k_x = 0$. Global analysis, which considers

disturbances varying in the streamwise direction, leads to results with valuable information about the evolution of streaks, and provides a framework for comparison with spectral proper orthogonal decomposition modes. Similar tools have been used in turbulent jets to identify Kelvin-Helmholtz wavepackets [20–22], and the application of these tools may provide new understanding on the role of the lift-up effect in jets.

This paper focuses on the application of the aforementioned method to turbulent jets, so as to model large-scale streaky structures in the velocity field. We perform global resolvent analysis focusing on low Strouhal numbers and compare with spectral proper orthogonal decomposition from a $M = 0.4$ turbulent jet. The results lead to conclusions about the optimal forcing that generates streaks, which we consider in the framework of the lift-up effect. The remainder of the paper is organised as follows: in section II, we describe the mathematical formulation of global resolvent analysis and spectral proper orthogonal decomposition (SPOD), where some details about the numerical computations are also provided. This is followed by the analysis of SPOD and global resolvent results (in section III) for several azimuthal wavenumbers, where a mechanism for the generation of streaks is proposed. The paper is then closed by a summary of the main conclusions in section IV.

II. Mathematical model

A. Spectral Proper Orthogonal Decomposition

Spectral proper orthogonal decomposition (SPOD) aims at identifying the most energetic coherent structures in a given database. To do so, we firstly decompose the turbulent field in temporal mean and fluctuation as

$$\tilde{\mathbf{u}}(\mathbf{x}, t) = \mathbf{U}(\mathbf{x}) + \mathbf{u}'(\mathbf{x}, t) \quad (1)$$

where $\mathbf{x} = (x, r, \theta)$. Afterwards, we Fourier transform the fluctuations in time and azimuth. Following [1, 23], we can write the SPOD integral equation as:

$$\int_{\Omega} R(x, x', r, r', m, \omega) \xi(x', r', m, \omega) r' dr' dx' = \sigma(m, \omega) \xi(x, r, m, \omega) \quad (2)$$

where R is the two-point cross-spectral tensor of the velocity fluctuations. Equation 2 is an eigenvalue problem, where σ is the eigenvalue and ξ is the corresponding eigenfunction. As the cross-spectral tensor is Hermitian, eigenvalue problem leads to real eigenvalues σ (each of them proportional to the energy of the mode), and orthonormal eigenfunctions ξ , which define the shape of the modes. It is shown by [20] that the SPOD modes should match the resolvent modes if the non-linear forcing is white noise in space, which gives us ground for the comparison between these two analyses.

The SPOD is applied to the same database studied in [11, 24]. Dual-plane time-resolved stereoscopic particle image velocimetry (PIV) was used to obtain the cross-spectral matrix for each azimuthal wavenumber for a $Re = 4.6 \times 10^5$ turbulent jet with Mach $M = 0.4$. The instantaneous velocity fields were interpolated onto a polar grid for $r/D \leq 0.8$, and the axial positions of the PIV planes (x_1, x_2) were varied between $1 \leq x_1/D \leq 8$ and $x_1/D \leq x_2/D \leq 8$, with spacing $\Delta x = 0.5D$. The cross-spectral density (CSD) matrix of the PIV data is obtained using the Welch periodogram technique with blocks of $n_{fft} = 128$ samples, with overlap of 50%. A standard Hann tapering window was applied to all blocks of data to minimise spectral leakage. More details on the experimental setup and on the data processing can be found in [24].

B. Resolvent Analysis

The resolvent analysis focuses on finding forcings that will lead to the most amplified response in the flow. By analysing forcing and response modes, we can gather information about the relevant structures inside the turbulent media and the forces that would generate them. Following the formulation from Schmidt *et al.* [22], we can rearrange the equations, leading to the linearised Navier-Stokes system in the input-output form:

$$\frac{\partial \mathbf{q}}{\partial t} = \mathbf{L}\mathbf{q} + \mathbf{B}\mathbf{f} \quad (3)$$

$$\phi = \mathbf{C}\mathbf{q}, \quad (4)$$

where all quantities are Fourier transformed in azimuth (m is the azimuthal wavenumber), $\mathbf{q}(x, r, m, t)$ is the state vector, which is a function of the flow variables, and $\mathbf{f}(x, r, m, t)$ is the forcing term, which is considered to gather the non-linear

terms. Equation 3 describes the time evolution of the disturbances by the operator L , and equation 4 defines the output of the system $\phi(x, r, m, t)$. Assuming that the linear operator L is stable, we can merge these equations in order to obtain a frequency response function between input and output. By further Fourier transforming these quantities in time, one can write

$$[-i\omega I - L]\hat{\mathbf{q}} = \mathbf{B}\hat{\mathbf{f}} \quad (5)$$

$$\Rightarrow \hat{\mathbf{q}} = [-i\omega I - L]^{-1}\mathbf{B}\hat{\mathbf{f}}, \quad (6)$$

which leads to

$$\hat{\phi} = \mathbf{C}[-i\omega I - L]^{-1}\mathbf{B}\hat{\mathbf{f}} = \mathbf{R}\hat{\mathbf{f}}, \quad (7)$$

where the resolvent operator is given by $\mathbf{R} = \mathbf{C}[-i\omega I - L]^{-1}\mathbf{B}$, and the “hats” indicate Fourier transformed variables. By performing a singular value decomposition (SVD) of this operator, one can find the optimal forcing $\hat{\mathbf{f}}$ of the flow so that

$$s_1^2 = \max_f \left\{ \frac{\langle \mathbf{R}\hat{\mathbf{f}}, \mathbf{R}\hat{\mathbf{f}} \rangle}{\langle \hat{\mathbf{f}}, \hat{\mathbf{f}} \rangle} \right\}, \quad (8)$$

where s_1 is the gain related to the most amplified forcing, or the first singular mode.

This formulation is implemented numerically as in [22]. The computations were performed in MATLAB, with the resolvent operator built to ensure the energy norm in the SVD computations. Since the forcing term is considered to combine the non-linear terms of the linearised Navier-Stokes equations, a weight matrix is implemented to benefit regions where the turbulent kinetic energy (computed from a large-eddy simulation) is higher. All computations were performed for a $M = 0.4$ jet, with mean flow derived from the same large-eddy simulation, for $Re = 3 \times 10^4$ and $St = 0.05$. Since SPOD was evaluated for $x/D \leq 8$, we restrict the domain to a similar region ($0 \leq x/D \leq 10$), and a sponge zone is implemented between $10 \leq x/D \leq 14$ and between $-1 \leq x/D \leq 0$. With this domain, we focus on the forcings and responses related to the dominant mechanism in regions closer to the nozzle ($x/D \leq 10$), which is also the region where SPOD seeks the most energetic structures. Therefore, both analyses concern the structures generated where linear mechanisms are important, especially for the generation of coherent structures that might play a role in the jet dynamics.

III. Results

The main objective of this work is to study the lift-up mechanism in a turbulent jet. Therefore, considering that this phenomenon is more clearly seen in the low frequency range, we performed the analysis for non-dimensional frequency $St = 0.05$, due to the high computational cost of performing global resolvent computations for $St = 0$. Spectral proper orthogonal decomposition (SPOD) modes are also evaluated at this frequency, and, although the Reynolds number in both analyses differ, this method will provide a reference for comparison with resolvent modes. It is known from [20] that SPOD and resolvent modes should match if the forcing term is uncorrelated in space, which can be a strong assumption for a turbulent flow. However, if the optimal forcing has a gain much larger than suboptimal ones, flow fluctuations are dominated by the optimal response [20, 25]; thus, resolvent analysis has been useful in the determination of the underlying mechanisms in wall-bounded [15, 17] and free-shear flows [20–22, 26], encouraging the application of the method for this flow to better understand the role of the lift-up effect in a turbulent jet.

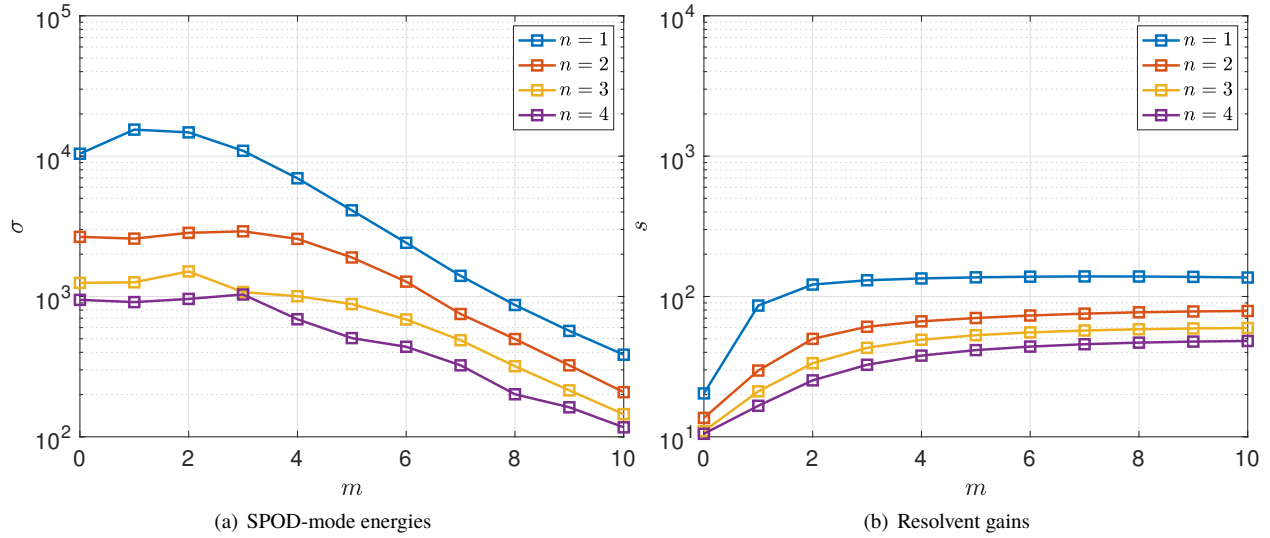


Figure 1 First four SPOD energies and resolvent gains for several azimuthal modes and $St = 0.05$.

The SPOD-mode energies for the first 4 modes is shown in figure 1(a), showing a dominance of the first mode in the low azimuthal wavenumber region, with the difference between optimal and suboptimal decreasing as we shift to higher values of m . This dominance is usually related to a preeminence of a physical mechanism (such as the Kelvin-Helmholtz instability or the lift-up effect); in [11], the same dominance was identified for $St = 0$, with gains peaking at $m = 3$. Further analysis led to the conclusion that the coherent structure related to that peak was a low-azimuthal wavenumber streak. For the present case, though, this dominance for resolvent gains is not as strong, and there are several differences between the two curves. First, while the gains decrease as we increase the values of m for the SPOD, resolvent gains almost reach a plateau for higher azimuthal wavenumbers. There are some possible reasons for this difference: in the experiment, some of the forcing may be localised inside the nozzle (including a turbulent boundary layer, which is also dominated by streaks), which is not included in the resolvent calculation. This can provide a more effective forcing for low-order azimuthal modes. Another possibility is that the spatial white-noise assumption for the forcing is too strong for this flow. If that is the case, the azimuthal spectrum of the non-linear term of the flow can cause low-order azimuthal modes to be forced more strongly than higher ones.

In some sense, the results shown in figure 1(a,b) are similar to what was found by [26] concerning the behaviour of optimals and suboptimals as a function of frequency. As in the previous work, the two curves can be very different from each other and still point to the same mechanism (in their case, the Kelvin-Helmholtz instability). In this case, the differences might be related to the assumptions of the resolvent model, such as the enforcement of uncorrelated forcing in space (with the same amplitude for all m), and the weight matrix in the resolvent analysis, which benefits regions with higher turbulent kinetic energy, a feature not yet implemented in the SPOD computations. Also, SPOD was computed using only the streamwise component of the velocity, while resolvent analysis takes into account all velocity components for the energy norm. Another possibility is the Reynolds numbers difference between the two cases, which could also explain the difference in amplitude of the gains, since resolvent gains scale with Re^2 for the lift-up mechanism [14]. Nevertheless, the gains from both analyses are related to elongated structures in the streamwise direction, as is shown in figure 2.

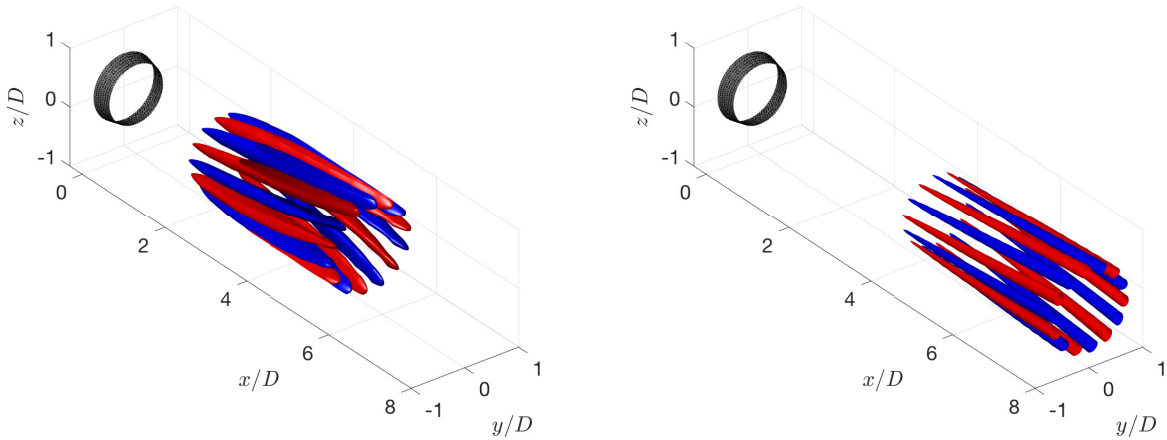


Figure 2 Isocontours of 40% of the real part of the first SPOD mode (left) and first resolvent mode (right) for $St = 0.05$ and $m = 7$ (streamwise component).

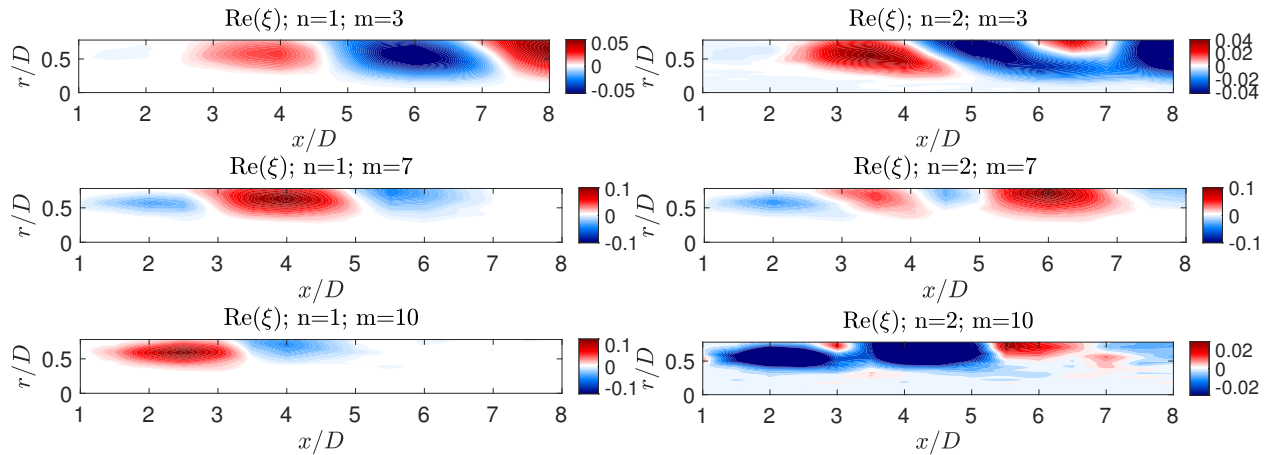


Figure 3 Real part of the first (left) and second (right) SPOD modes for $St = 0.05$ and several azimuthal modes (streamwise component).

We now focus on the analysis of the shapes of the resolvent and SPOD modes. For that, three wavenumbers were chosen as representative of the phenomenon we want to analyse: $m = 3$ is the peak wavenumber of streaks for this turbulent jet (from [11]); $m = 7; 10$ are wavenumbers whose SPOD modes have higher amplitudes in the region upstream of the jet; also, the streaky behaviour of the disturbances is clearer for these last cases. The shape of the streamwise component of the two first SPOD modes for these wavenumbers can be seen in figure 3. The first feature shown in all modes of figure 3 is their wavy behaviour in the streamwise direction; since we are looking at non-zero frequency, a non-zero azimuthal phase velocity induces oscillations in the (x, r) plane, which will lead to slightly rotating streaks in the field. This is more clearly seen in figure 2(a), where isosurfaces of 40% of the streamwise velocity for $m = 7$ are shown, highlighting the streaky behaviour of these structures. Some other features of figure 3 are similar to the findings reported in [11], especially the decrease in size of the streaks (in both axial and radial direction) and their movement towards the nozzle/lipline for increasing m . The second SPOD mode keep these characteristics, but it also displays a higher number of oscillations in the streamwise direction, which is a reflex of a higher twist of the streaks in azimuth, leading to streaks with stronger variation in the azimuthal direction. This can also be related to the meandering motion of streaks [9]; since this is a secondary effect on the structures, it is here identified in the second and higher order SPOD modes.

The structure of the first response mode in resolvent analysis is the quantity that can be compared with the first SPOD mode. The streamwise component of the response u is depicted together with the radial component of the forcing

f_r in figure 4. These components (together with the azimuthal component of the forcing) are the most relevant for this frequency-wavenumber combinations (the streamwise component of the forcing, for instance, is one order of magnitude lower for these cases, similarly for the other components of the response). These are also representative of the lift-up effect, where streaks of streamwise velocity are forced by streamwise vortices (forcing in the radial and azimuthal directions). The oscillations found in the SPOD modes are also present for this case, keeping the characteristic swirl of these streaks (as also shown in figure 2(b)). The response modes also follow some of the trends identified for the SPOD modes, with structures more and more concentrated radially in the lipline. Still, there are clear differences between SPOD and resolvent modes, especially concerning their radial and axial support. Response modes are rather concentrated in the lipline, which is expected due to the higher shear in that region, and much more spread in the streamwise direction. The Reynolds number can change the spatial support of the modes due to the molecular diffusion mechanism, but a decrease in Reynolds would also damp the mechanism. One possibility is that this difference is related to the restriction applied to the forcing (via turbulent kinetic energy values), but it is more likely linked with the assumption of uncorrelated forcing in space. Previous works [27] have shown that standard resolvent analysis can provide results more concentrated spatially than the expected, an effect that can be remediable with the inclusion of an eddy viscosity, which would be equivalent to considering a covariance of the forcing different from the identity in the standard linearised Navier-Stokes system, with molecular viscosity. The statistics of the non-linear terms in the real flow might be the main source of divergence between both analyses, since the spatial evolution of the turbulent boundary layer inside the nozzle is not taken into account in the resolvent.

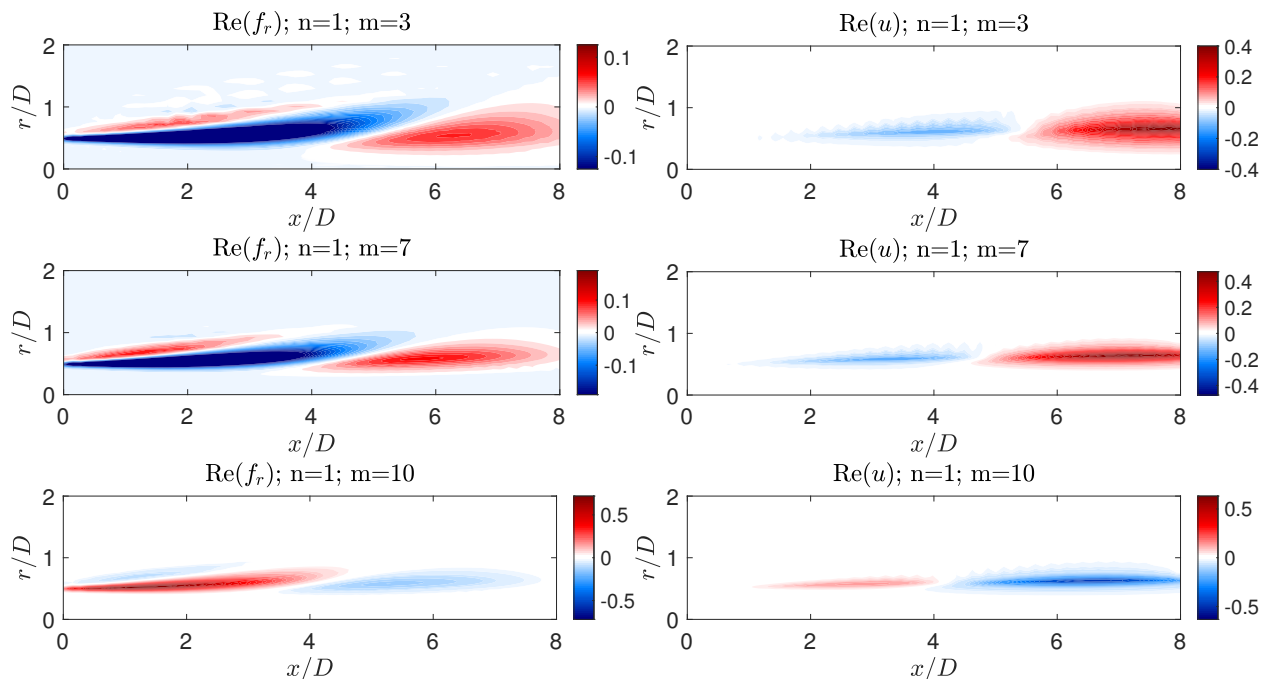


Figure 4 First resolvent mode for $St = 0.05$ and several azimuthal modes. Real part of the radial component of the forcing (left) and real part of the streamwise component of the response (right) are shown.

With those differences clear, we can analyse more closely the new information brought by resolvent analysis: the shapes of the forcing term and the other velocity components. First column of figure 4 shows the radial component of the forcing mode for several values of m . Most of the remarks regarding the response modes are also valid here, since the forcing follows the same behaviour of diminishing the spatial extent as the azimuthal wavenumber is increased. The location of the forcing, on the other hand, is quite different from the response. Figure 4 shows that the forcing is always located upstream from the response, starting close to the nozzle. Furthermore, when the amplitude of the forcing starts to decrease, the amplitude of the streaks starts to grow, pointing to a sequence of events related to the formation of these structures. Such sequence is similar to the lift-up effect in transitional boundary layers [15], which points out that a similar mechanism is active in turbulent jets.

The overlapping region between forcing and response also provides a relevant information (which can be seen more

clearly of the $m = 10$ case): streaks of positive (respectively negative) u component are always associated with positive (respectively negative) radial forcing. This corroborates the hypothesis that these structures are related to the lift-up effect, since positive streaks are regions where flow is transferred radially from high-speed regions (in this case, the core of the jet) to low-speed regions, a phenomenon induced by the formation of streamwise vortices.

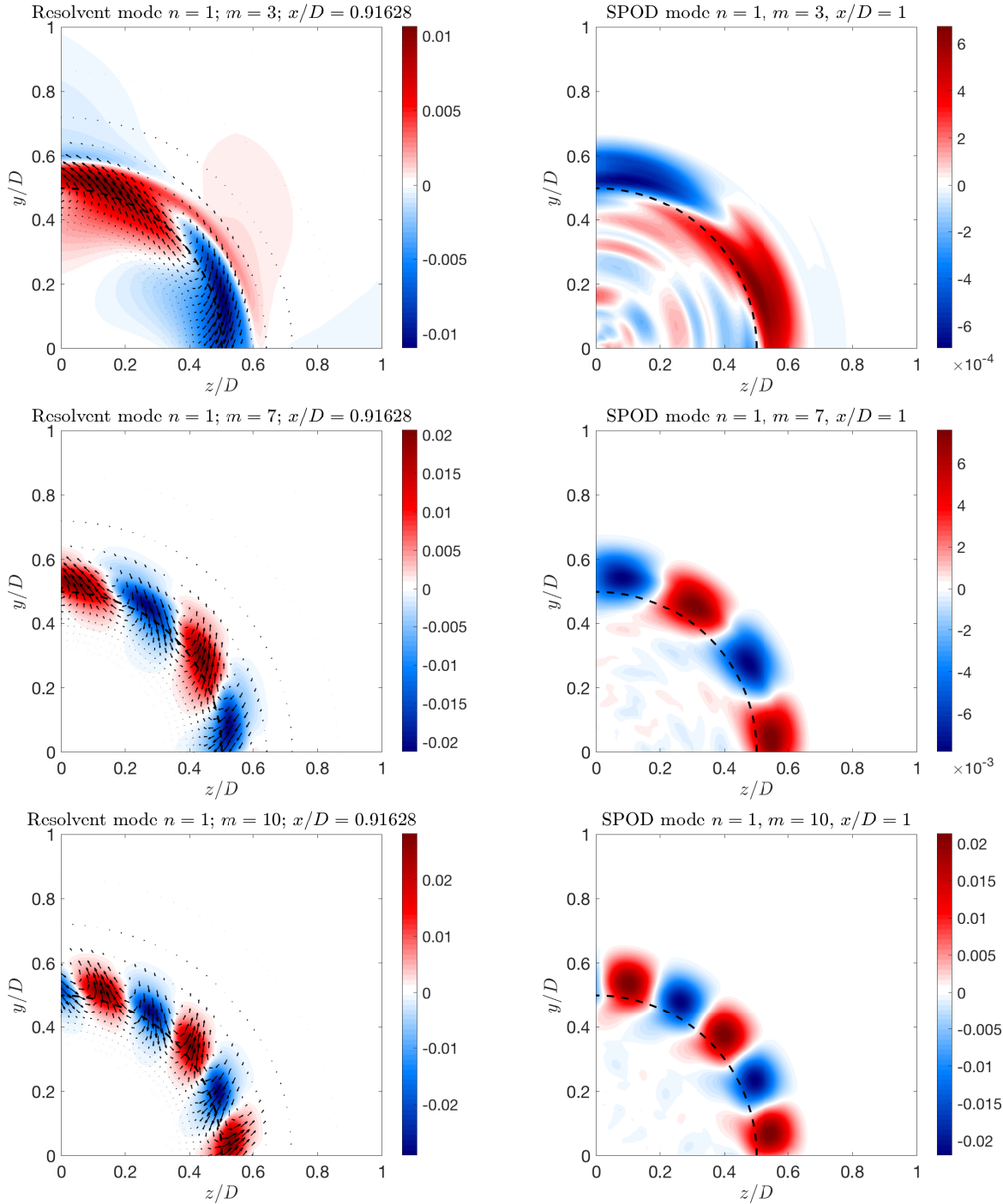


Figure 5 Streamwise component of the first resolvent response mode (left) and streamwise component of the first SPOD mode (right) for several azimuthal wavenumbers and $x/D = 1$ (shown in colors). Radial and azimuthal components of the respective forcing mode is also depicted with the response mode (arrows). The dashed line indicates the position of the lipline.

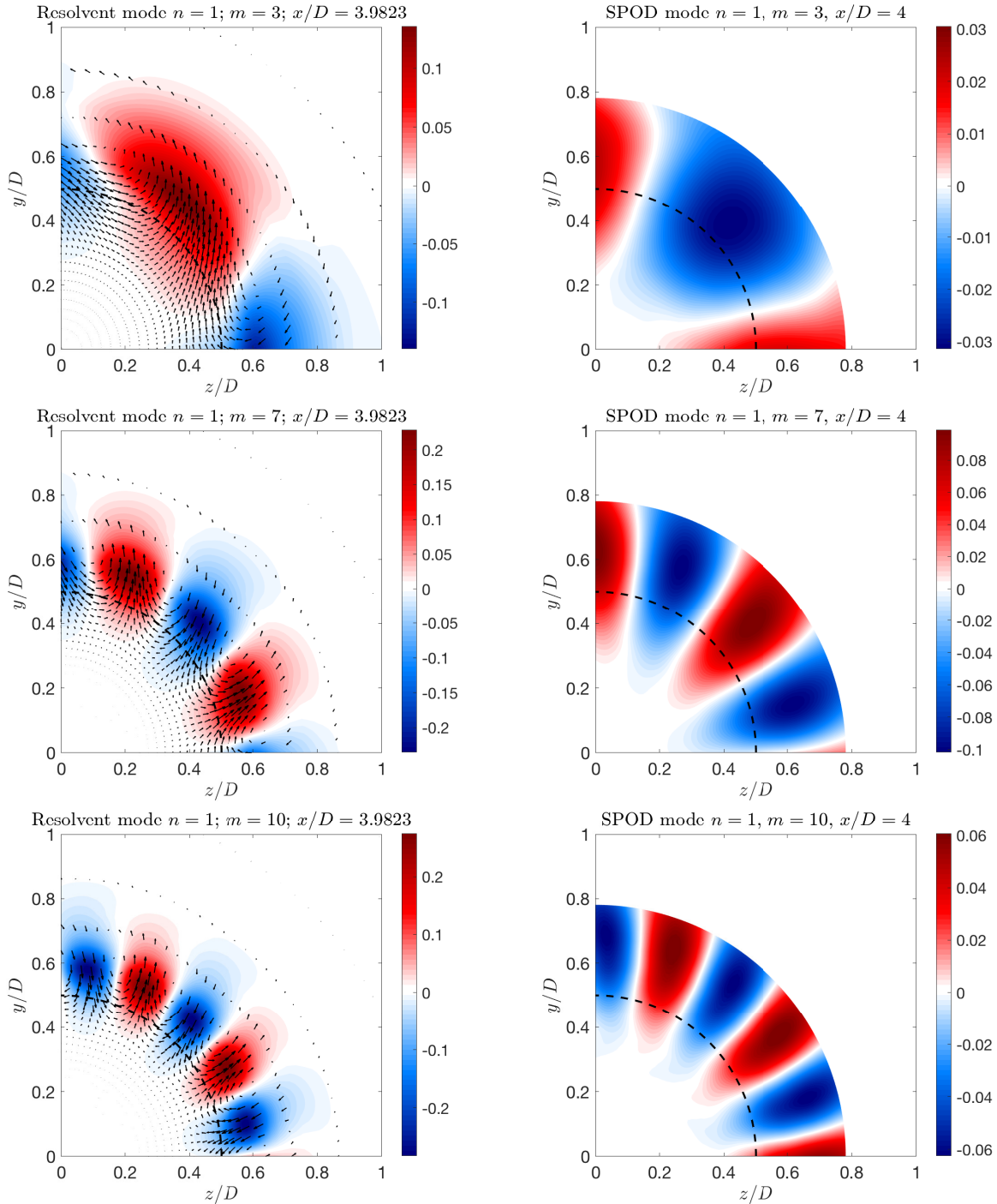


Figure 6 Streamwise component of the first resolvent response mode (left) and streamwise component of the first SPOD mode (right) for several azimuthal wavenumbers and $x/D = 4$ (shown in colors). Radial and azimuthal components of the respective forcing mode is also depicted with the response mode (arrows). The dashed line indicates the position of the lipline.

The structure of the forcing and its relation to the response modes can be better understood by looking at axial slices of the jet. Figure 5 shows the streamwise component of the response and SPOD modes for $x/D = 1$ and several azimuthal wavenumbers, with the forcing at the given station depicted by the arrows. Looking at this specific axial position, resolvent and SPOD modes have similar structures for all cases, with streamwise velocities peaking at positions

close to the lipline. A possible reason for that is that, in the near-nozzle region, the lower characteristic scales of turbulent structures are much smaller than the streak size, and thus the forcing may be approximated as spatially white, leading to a good agreement between SPOD and response modes. Further downstream the increase of length scales leads to a correlated forcing, and the agreement deteriorates. This effect can be seen in figure 6, which shows the same quantities for $x/D = 4$. At this position, the agreement between SPOD and resolvent deteriorates, and the SPOD modes start to have a higher radial support, while resolvent modes, although with some increase in the radial extent, are still concentrated in regions close to the lipline.

The arrows in figures 5 and 6 represent the radial and azimuthal components of the forcing mode at each axial station. These plots confirm the trend identified in figure 4: whenever a positive streak appear in the flow, it is related to a forcing that tends to transfer flow from high to low speed regions. The novelty brought by this representation is the direction in which this phenomenon occur. For all cases, the forcing seems to follow the swirl of the streaks, and is more inclined in the azimuthal direction as m decreases. For $m = 3$, for instance, the forcing acts almost tangentially to the lipline (represented by the dashed line), while it is almost radial at the streak positions for $m = 10$. Figures 5 and 6 also helps the understanding of how the direction of the radial velocity is related to streamwise vortices: two streaks in opposite directions are related to perpendicular forcings, also opposed to each other, and these are linked by the azimuthal component of $\hat{\mathbf{f}}$ in the inner and outer parts of the jet. The final picture shown in figure 6 for $m = 10$, for instance, is of several vortices alternating with the streaks, with a center slightly away from the streak peak, with radial support following the growth of the streaks.

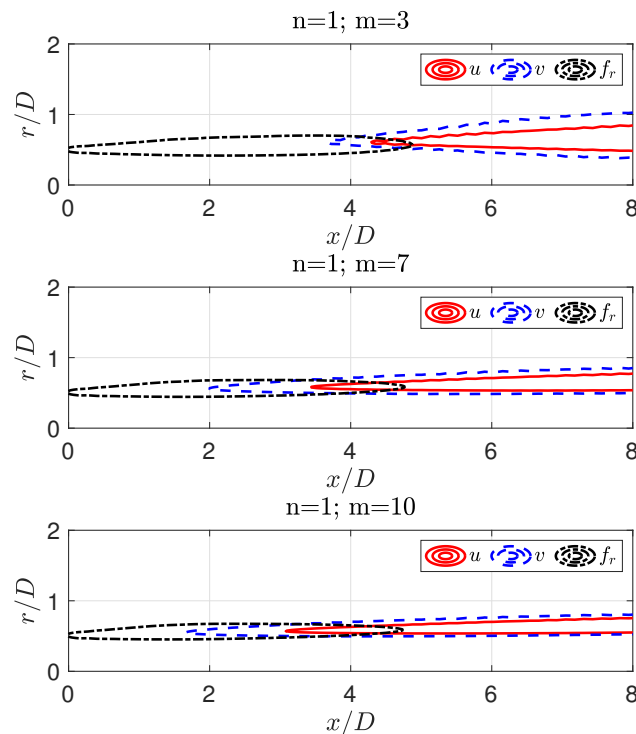


Figure 7 Contours of 30% of the maximum of the absolute value of streamwise and radial components of the first response mode, and radial component of the first forcing mode for several azimuthal wavenumbers.

Even though the present analysis is in the frequency domain (focusing on low frequencies), the different positions of the forcing and response in figure 4 also provide an indication of the dynamics beneath the formation of streaks. As seen in [13], transient growth analysis of wall bounded flows show that the optimal initial disturbances that generate streamwise streaks are streamwise vortices (for the unforced problem). As the disturbances evolve in time, these vortices are slowly damped, while the streaks are formed and continuously reinforced. The final picture (at the time of maximal growth) is a flow marked by the presence of high amplitude streaks, with some reminiscences of the vortices. Since we are dealing with a spatially varying flow, we expect that a similar dynamics would occur here, but with the streamwise coordinate as a surrogate for time. In figure 4, we can see a vortical forcing (represented by the radial component

of the forcing) upstream and the generated streaks downstream. In figure 7, the absolute value of these quantities is plotted with the response vortices (embodied by the radial component of the velocity v), where a contour of 30% of the maximum is shown for each structure. For all values of m , the forcing is located virtually in the same position, close to the nozzle. The main difference is on the position where the vortices and streaks are generated: for all cases, the vortices experience a growth upstream of the appearance of streaks, with the difference between the starting point of both structures increasing for higher azimuthal wavenumbers. Based on that, we propose the following sequence of events for the generation of streaks in this turbulent jet: (1) the non-linearities from the turbulence in the near-nozzle region (which come from a turbulent boundary layer) find a projection in the optimal forcing mode, triggering the mechanism; (2) this forcing generates streamwise vortices in the flow in regions closer to the nozzle; and (3) these vortices progressively generate the downstream streaks via the lift-up mechanism. We highlight that the described dynamics is supported by the present results, but further studies on turbulent jets are needed to confirm this theory. Other tools, such as spatial transient growth and adjoint based optimisation [16] can also be used to evaluate the validity of this mechanism.

IV. Conclusion

We have analysed resolvent computations for a turbulent jet at $M = 0.4$, comparing with results from spectral proper orthogonal decomposition. The analysis was performed in the low frequency region ($St = 0.05$), where the lift-up mechanism is known to be relevant. The results show that streaks are, indeed, present in the turbulent field of the jet, and that they swirl for non-zero frequencies. A study of the spatial extent of the streaks was also performed using both SPOD and resolvent analyses, leading to the conclusion that, as the azimuthal wavenumber increases, the spatial support of the structures decreases, such that, for higher values of m , streaks are more concentrated around the lipline and closer to the nozzle. Resolvent analysis also led to important conclusions about the optimal forcing that generate streaks in this case: as usual in flows dominated by the lift-up effect, the optimal forcing takes the form of streamwise vortices. For these swirling streaks, the vortices are also spinning at the same rate, leading to slightly tilted structures for low azimuthal wavenumber. Finally, the fact that the forcing is always located upstream of the streaks suggests a simple mechanism for the generation of these based on transient-growth analysis, where vortices in the velocity field are excited by the non-linearities of the flow, being amplified and, thus, generating streaks downstream.

Acknowledgments

Petrônio Nogueira was funded by a CNPq scholarship. André Cavalieri acknowledges financial support by CNPq (grant number 310523/2017-6). This study was financed in part by the Coordenação de Aperfeiçoamento de Pessoal de Nível Superior - Brasil (CAPES) - Finance Code 001.

References

- [1] Cavalieri, A. V. G., Rodríguez, D., Jordan, P., Colonius, T., and Gervais, Y., "Wavepackets in the velocity field of turbulent jets," *Journal of Fluid Mechanics*, Vol. 730, 2013, pp. 559–592. doi:10.1017/jfm.2013.346, URL http://journals.cambridge.org/article_S0022112013003467.
- [2] Jordan, P., and Colonius, T., "Wave Packets and Turbulent Jet Noise," *Annual Review of Fluid Mechanics*, Vol. 45, No. 1, 2013.
- [3] Kline, S. J., Reynolds, W., Schraub, F., and Runstadler, P., "The structure of turbulent boundary layers," *Journal of Fluid Mechanics*, Vol. 30, No. 4, 1967, pp. 741–773.
- [4] Smits, A. J., McKeon, B. J., and Marusic, I., "High-Reynolds number wall turbulence," *Annual Review of Fluid Mechanics*, Vol. 43, 2011.
- [5] Hamilton, J. M., Kim, J., and Waleffe, F., "Regeneration mechanisms of near-wall turbulence structures," *Journal of Fluid Mechanics*, Vol. 287, 1995, pp. 317–348.
- [6] Waleffe, F., "Hydrodynamic Stability and Turbulence: Beyond Transients to a Self-Sustaining Process," *Studies in applied mathematics*, Vol. 95, No. 3, 1995, pp. 319–343.
- [7] Schoppa, W., and Hussain, F., "Coherent structure generation in near-wall turbulence," *Journal of fluid Mechanics*, Vol. 453, 2002, pp. 57–108.
- [8] Farrell, B. F., and Ioannou, P. J., "Dynamics of streamwise rolls and streaks in turbulent wall-bounded shear flow," *Journal of Fluid Mechanics*, Vol. 708, 2012, pp. 149–196.

- [9] Hutchins, N., and Marusic, I., “Evidence of very long meandering features in the logarithmic region of turbulent boundary layers,” *Journal of Fluid Mechanics*, Vol. 579, 2007, pp. 1–28.
- [10] Cossu, C., and Hwang, Y., “Self-sustaining processes at all scales in wall-bounded turbulent shear flows,” *Philosophical Transactions of the Royal Society A: Mathematical, Physical and Engineering Sciences*, Vol. 375, No. 2089, 2017, p. 20160088.
- [11] Nogueira, P. A., Cavalieri, A. V. G., Jordan, P., and Jaunet, V., “Large-scale, streaky structures in turbulent jets,” *Journal of Fluid Mechanics*, Vol. in press, 2019.
- [12] Ellingsen, T., and Palm, E., “Stability of linear flow,” *The Physics of Fluids*, Vol. 18, No. 4, 1975, pp. 487–488.
- [13] Butler, K. M., and Farrell, B. F., “Three-dimensional optimal perturbations in viscous shear flow,” *Physics of Fluids A: Fluid Dynamics*, Vol. 4, No. 8, 1992, pp. 1637–1650.
- [14] Schmid, P. J., and Henningson, D. S., *Stability and transition in shear flows*, Vol. 142, Springer Science & Business Media, 2012.
- [15] Monokrousos, A., Åkervik, E., Brandt, L., and Henningson, D. S., “Global three-dimensional optimal disturbances in the Blasius boundary-layer flow using time-steppers,” *Journal of Fluid Mechanics*, Vol. 650, 2010, pp. 181–214.
- [16] Levin, O., and Henningson, D. S., “Exponential vs algebraic growth and transition prediction in boundary layer flow,” *Flow, Turbulence and Combustion*, Vol. 70, No. 1-4, 2003, pp. 183–210.
- [17] Brandt, L., Sipp, D., Pralits, J. O., and Marquet, O., “Effect of base-flow variation in noise amplifiers: the flat-plate boundary layer,” *Journal of Fluid Mechanics*, Vol. 687, 2011, pp. 503–528.
- [18] Jovanovic, M. R., and Bamieh, B., “Componentwise energy amplification in channel flows,” *Journal of Fluid Mechanics*, Vol. 534, 2005, pp. 145–183.
- [19] McKeon, B., and Sharma, A., “A critical-layer framework for turbulent pipe flow,” *Journal of Fluid Mechanics*, Vol. 658, 2010, pp. 336–382.
- [20] Towne, A., Schmidt, O. T., and Colonius, T., “Spectral proper orthogonal decomposition and its relationship to dynamic mode decomposition and resolvent analysis,” *Journal of Fluid Mechanics*, Vol. 847, 2018, pp. 821–867.
- [21] Semeraro, O., Jaunet, V., Jordan, P., Cavalieri, A. V., and Lesshafft, L., “Stochastic and harmonic optimal forcing in subsonic jets,” *22nd AIAA/CEAS Aeroacoustics Conference*, 2016, p. 2935.
- [22] Schmidt, O. T., Towne, A., Rigas, G., Colonius, T., and Brès, G. A., “Spectral analysis of jet turbulence,” *Journal of Fluid Mechanics*, Vol. 855, 2018, pp. 953–982.
- [23] Jung, D., Gamard, S., and George, W. K., “Downstream evolution of the most energetic modes in a turbulent axisymmetric jet at high Reynolds number. Part 1. The near-field region,” *Journal of Fluid Mechanics*, Vol. 514, 2004, pp. 173–204.
- [24] Jaunet, V., Jordan, P., and Cavalieri, A., “Two-point coherence of wave packets in turbulent jets,” *Physical Review Fluids*, Vol. 2, No. 2, 2017, p. 024604.
- [25] Cavalieri, A., Jordan, P., and Lesshafft, L., “Wave-packet models for jet dynamics and sound radiation,” *Applied Mechanics Reviews*, 2019.
- [26] Lesshafft, L., Semeraro, O., Jaunet, V., Cavalieri, A. V., and Jordan, P., “Resolvent-based modelling of coherent wavepackets in a turbulent jet,” *Physical Review Fluids*, Vol. in press, 2019.
- [27] Morra, P., Semeraro, O., Henningson, D. S., and Cossu, C., “On the relevance of Reynolds stresses in resolvent analyses of turbulent wall-bounded flows,” *arXiv preprint arXiv:1901.04356*, 2019.